



The Absolute Chronology and Thermal Processing of Solids in the Solar Protoplanetary Disk

James N. Connelly *et al.*

Science **338**, 651 (2012);

DOI: 10.1126/science.1226919

This copy is for your personal, non-commercial use only.

If you wish to distribute this article to others, you can order high-quality copies for your colleagues, clients, or customers by [clicking here](#).

Permission to republish or repurpose articles or portions of articles can be obtained by following the guidelines [here](#).

The following resources related to this article are available online at www.sciencemag.org (this information is current as of November 1, 2012):

Updated information and services, including high-resolution figures, can be found in the online version of this article at:

<http://www.sciencemag.org/content/338/6107/651.full.html>

Supporting Online Material can be found at:

<http://www.sciencemag.org/content/suppl/2012/11/01/338.6107.651.DC1.html>

This article **cites 48 articles**, 9 of which can be accessed free:

<http://www.sciencemag.org/content/338/6107/651.full.html#ref-list-1>

Downloaded from www.sciencemag.org on November 1, 2012

12. E. Sperotto, G. P. M. van Klink, G. van Koten, J. G. de Vries, *Dalton Trans.* **39**, 10338 (2010).
13. J. W. Tye, Z. Weng, A. M. Johns, C. D. Incarvito, J. F. Hartwig, *J. Am. Chem. Soc.* **130**, 9971 (2008).
14. R. Giri, J. F. Hartwig, *J. Am. Chem. Soc.* **132**, 15860 (2010).
15. G. O. Jones, P. Liu, K. N. Houk, S. L. Buchwald, *J. Am. Chem. Soc.* **132**, 6205 (2010).
16. H.-Z. Yu, Y.-Y. Jiang, Y. Fu, L. Liu, *J. Am. Chem. Soc.* **132**, 18078 (2010).
17. S. Natarajan, S. H. Kim, *Chem. Commun. (Camb.)* **7**, 729 (2006).
18. S. Natarajan, G. Liu, S. H. Kim, *J. Phys. Chem. B* **110**, 8047 (2006).
19. S. B. Harkins, J. C. Peters, *J. Am. Chem. Soc.* **127**, 2030 (2005).
20. J. C. Deaton *et al.*, *J. Am. Chem. Soc.* **132**, 9499 (2010).
21. K. J. Lotito, J. C. Peters, *Chem. Commun. (Camb.)* **46**, 3690 (2010).
22. R. A. Rossi, *Acc. Chem. Res.* **15**, 164 (1982).
23. J. M. R. Narayanan, C. R. J. Stephenson, *Chem. Soc. Rev.* **40**, 102 (2011).
24. D. A. Nicewicz, D. W. C. MacMillan, *Science* **322**, 77 (2008).
25. Materials and methods are available as supplementary materials on *Science Online*.
26. Z. Xi, F. Liu, Y. Zhou, W. Chen, *Tetrahedron* **64**, 4254 (2008).
27. N. P. Mankad, W. E. Antholine, R. K. Szilagy, J. C. Peters, *J. Am. Chem. Soc.* **131**, 3878 (2009).
28. R. J. Enemærke, T. B. Christensen, H. Jensen, K. Daasbjerg, *J. Chem. Soc. Perkin Trans. 2* **9**, 1620 (2001).
29. C. L. Keller, J. D. Dalessandro, R. P. Hotz, A. R. Pinhas, *J. Org. Chem.* **73**, 3616 (2008).
30. R. L. Dannley, E. C. Gregg Jr., R. E. Phelps, C. B. Coleman, *J. Am. Chem. Soc.* **76**, 445 (1954).
31. E. I. Solomon, *Inorg. Chem.* **45**, 8012 (2006).
32. M. Hay, J. H. Richards, Y. Lu, *Proc. Natl. Acad. Sci. U.S.A.* **93**, 461 (1996).
33. A. Annunziata, C. Galli, M. Marinelli, T. Pau, *Eur. J. Org. Chem.* **2001**, 1323 (2001).

Acknowledgments: This work was supported by the National Science Foundation (graduate research fellowships for S.E.C. and K.J.L.) and by the Gordon and Betty Moore Foundation. Metrical parameters for the structure of copper complex **1** are available free of charge from the Cambridge Crystallographic Data Centre under reference CCDC-896019.

Supplementary Materials

www.sciencemag.org/cgi/content/full/338/6107/647/DC1
Materials and Methods
Figs. S1 to S41
Tables S1 to S3
References (34–46)

22 June 2012; accepted 10 September 2012
10.1126/science.1226458

The Absolute Chronology and Thermal Processing of Solids in the Solar Protoplanetary Disk

James N. Connelly,^{1*} Martin Bizzarro,^{1*} Alexander N. Krot,^{1,2} Åke Nordlund,³ Daniel Wielandt,¹ Marina A. Ivanova⁴

Transient heating events that formed calcium-aluminum-rich inclusions (CAIs) and chondrules are fundamental processes in the evolution of the solar protoplanetary disk, but their chronology is not understood. Using U-corrected Pb-Pb dating, we determined absolute ages of individual CAIs and chondrules from primitive meteorites. CAIs define a brief formation interval corresponding to an age of 4567.30 ± 0.16 million years (My), whereas chondrule ages range from 4567.32 ± 0.42 to 4564.71 ± 0.30 My. These data refute the long-held view of an age gap between CAIs and chondrules and, instead, indicate that chondrule formation started contemporaneously with CAIs and lasted ~ 3 My. This time scale is similar to disk lifetimes inferred from astronomical observations, suggesting that the formation of CAIs and chondrules reflects a process intrinsically linked to the secular evolution of accretionary disks.

The only record of our solar system's formative stages comes from the earliest solids preserved from the protoplanetary disk that now reside as millimeter- to centimeter-sized objects—calcium-aluminum-rich inclusions (CAIs) and chondrules—in chondrite meteorites. These complex objects have been the subject of intense study in an attempt to decipher their origins and, in turn, use them as records of the dynamics of the protoplanetary disk that led to the formation of the solar system (1–8). Most CAIs formed as fine-grained condensates from a gas of approximately solar composition in a high-temperature environment (>1300 K) at total pressure $\leq 10^{-4}$ bar, with a subset experiencing re-melting to form distinct coarser igneous tex-

tures (9). In contrast, most chondrules represent coalesced dust aggregates that were subsequently rapidly melted and cooled in lower-temperature regions (<1000 K) and higher ambient vapor pressures ($\geq 10^{-3}$ bar) than CAIs, resulting in igneous porphyritic textures (10). Despite their formation by different mechanisms (condensation versus dust accretion) in distinct environments (11), these objects share common histories of exposure to brief, high-temperature events at least once in their respective evolutions.

The current perception of the relative timing of CAI and chondrule formation is based on the short-lived ^{26}Al - ^{26}Mg chronometer [^{26}Al decays to ^{26}Mg with a half-life of 0.73 million years (My)], which has led to a growing consensus that chondrules formed 1 to 2 My after CAIs (12). This age difference has long been used as a central observation in defining models of chondrule formation and, in addition, implies that the melting of CAIs and chondrules was produced by different mechanisms and/or heat sources. However, the ^{26}Al - ^{26}Mg dating method critically depends on the disputed assumption of homogeneous distribution of ^{26}Al in space and time within the protoplanetary disk (13).

In contrast, chronologies based on long-lived radioisotope systems rely on the knowledge of the present-day abundances of the parent and daughter isotopes in a sample and therefore are free from assumptions of parent nuclide homogeneity. Of the various long-lived radioisotope systems, the Pb-Pb dating method is the most powerful tool to establish a high-resolution chronology of the first 10 My of the solar system. This chronometer is based on two isotopes of U, ^{238}U and ^{235}U , that decay in a chain to stable Pb isotopes, ^{206}Pb and ^{207}Pb , respectively, resulting in $^{207}\text{Pb}_R/^{206}\text{Pb}_R$ (where R = radiogenic) ratios that correspond to the amount of time passed since the system closed, by Eq. 1

$$\frac{^{207}\text{Pb}_R}{^{206}\text{Pb}_R} = \left(\frac{^{235}\text{U}}{^{238}\text{U}} \right) \left(\frac{(e^{\lambda_1 t} - 1)}{(e^{\lambda_2 t} - 1)} \right) \quad (1)$$

where λ_1 and λ_2 reflect the decay constants for ^{235}U and ^{238}U , respectively; t , time. The $^{207}\text{Pb}_R/^{206}\text{Pb}_R$ ratio of an inclusion is calculated by extrapolating from an array of measured Pb isotopic values that represent varying mixtures of radiogenic Pb and its initial Pb isotopic composition, which should approximate that of the solar system defined by the Nantan iron meteorite (14). However, attempts to date individual CAIs and chondrules by this approach have historically been frustrated by the difficulties in analyzing the small amounts of Pb in these inclusions. In addition, the $^{238}\text{U}/^{235}\text{U}$ ratio required for Eq. 1, which has traditionally been assumed to be 137.88 in all solar system materials, was demonstrated to vary in CAIs by 35ϵ units (deviations in parts per 10^4), corresponding to offsets in calculated Pb-Pb ages of up to 5 My (15). The observation of U isotope variability, attributed to the decay of the short-lived ^{247}Cm nuclide (^{247}Cm decays to ^{235}U with a half-life of 15.6 My) voided all published Pb-Pb ages for solar system materials that were based on an assumed $^{238}\text{U}/^{235}\text{U}$ ratio and made clear the need to have measurements of the U isotopic compositions for all materials dated by the Pb-Pb method.

To establish an assumption-free absolute chronology of CAI and chondrule formation, we have developed improved methods for the precise analysis of small amounts of Pb and U by thermal

¹Centre for Star and Planet Formation and Natural History Museum of Denmark, University of Copenhagen, DK-1350 Copenhagen, Denmark. ²Hawai'i Institute of Geophysics and Planetology, University of Hawai'i at Manoa, HI 96822, USA. ³Centre for Star and Planet Formation and Niels Bohr Institute, University of Copenhagen, DK-2100 Copenhagen, Denmark. ⁴Vernadsky Institute of Geochemistry and Analytical Chemistry, Moscow 119991, Russia.

*To whom correspondence should be addressed. E-mail: connelly@snm.ku.dk (J.N.C.); bizzarro@snm.ku.dk (M.B.)

ionization mass spectrometry and high-resolution inductively coupled plasma source mass spectrometry, respectively (16). We measured the $^{238}\text{U}/^{235}\text{U}$ ratios of three CAIs from the reduced CV chondrite Efremovka, three chondrules from the oxidized CV chondrite Allende, and whole-rock chondrites and differentiated meteorites in an attempt to understand the extent and origin of $^{238}\text{U}/^{235}\text{U}$ variations in the early solar system (Fig. 1 and Table 1). The Efremovka CAIs show a range of $^{238}\text{U}/^{235}\text{U}$ ratios (Table 1), confirming the presence of U isotope variability in refractory inclusions. In contrast, our analyses of meteorites derived from chondritic and differentiated asteroids as well as three individual chondrules from Allende show identical $^{238}\text{U}/^{235}\text{U}$ ratios within analytical uncertainty (Fig. 1), defining a weighted mean of 137.786 ± 0.013 . These observations indicate a uniform $^{238}\text{U}/^{235}\text{U}$ ratio in the inner solar system outside the CAI-forming region. This is consistent with an earlier study (17) but at odds with the solar system initial $^{247}\text{Cm}/^{235}\text{U}$ value of $\sim 1.1 \times 10^{-4}$ inferred from $^{238}\text{U}/^{235}\text{U}$ variability in Allende CAIs (15). Moreover, our analyses of Efremovka CAIs show significant departure from the apparent correlation between the $^{144}\text{Nd}/^{238}\text{U}$ [an assumed proxy for Cm/U (18)] and $^{235}\text{U}/^{238}\text{U}$ ratios of Allende CAIs (15), similarly to another recent study (19). Thus, we infer that the $^{238}\text{U}/^{235}\text{U}$ variability in CAIs largely reflects mass-dependent fractionation associated with the CAI-forming process and not ^{247}Cm decay (supplementary materials text 1).

The subset of chondrite meteorites we analyzed includes the Ivuna carbonaceous chondrite, a member of the rare clan of primitive meteorites referred to as CI chondrites. Composed of matrix material with the highest abundances of presolar grains, CI chondrites are generally considered to represent the least chemically fractionated and least thermally processed meteorites: They have solar abundances of most elements (20) and, by extension, have the solar $^{247}\text{Cm}/^{235}\text{U}$ ratio. Therefore, we interpret the $^{238}\text{U}/^{235}\text{U}$ value of 137.786 ± 0.013 obtained for bulk inner solar system materials as represent-

ing the best estimate of the bulk $^{238}\text{U}/^{235}\text{U}$ ratio of the solar system and hence that of the Sun.

To constrain the timing and duration of CAI and chondrule formation, we have obtained Pb isotope data for a suite of three CAIs from Efremovka (22E, 31E, and 32E), two ferromagnesian porphyritic olivine-pyroxene chondrules from Allende (C20 and C30), and three ferromagnesian porphyritic olivine (C1) and barred olivine-pyroxene chondrules (C2 and C3) from the unequilibrated ordinary chondrite NWA 5697. 22E is a fine-grained inclusion with a porous, nearly monomineralic hibonite core surrounded by a mantle composed of concentric zoned objects having a spinel-hibonite-perovskite core rimmed by the layers of melilite \pm anorthite and pyroxene. The texture and mineralogy of 22E indicate that it is an unmelted nebular condensate. 31E is a coarse-grained type B1 CAI with a pyroxene-melilite-spinel core surrounded by a melilite mantle and a multilayered Wark-Lovering rim sequence of spinel, melilite, pyroxene, and forsterite. 32E is a coarse-grained type B1 CAI with a melilite-pyroxene-anorthite-spinel core surrounded a melilite mantle, thin Wark-Lovering rim layers of pyroxene and spinel, and a forsterite-rich accretionary rim. Both coarse-grained CAIs experienced melting after their initial formation by condensation and evaporation processes. To calculate the Pb-Pb ages of the Efremovka CAIs, we used their measured $^{238}\text{U}/^{235}\text{U}$ ratios, which are characterized by a range of ~ 15 ϵ units (Table 1) with compositions that are both isotopically heavy and light relative to the bulk solar $^{238}\text{U}/^{235}\text{U}$ value of 137.786. The three CAIs yield ages of 4567.35 ± 0.28 My (22E), 4567.23 ± 0.29 My (31E), and 4567.38 ± 0.31 My (32E) (Table 1), with uncertainties including errors associated with both the Pb and U isotope measurements. The age concordancy of these inclusions, despite the wide range of their $^{238}\text{U}/^{235}\text{U}$ ratios, supports our interpretation that the $^{238}\text{U}/^{235}\text{U}$ variability was imparted during CAI formation and does not represent a secondary event such as, for example, mass-dependent fractionation resulting from variable redox conditions during alteration processes

on the CV chondrite parent body. The ages we report for Efremovka CAIs overlap with the age of 4567.18 ± 0.50 My recently obtained for the coarse-grained type B CAI SJ101 from Allende (19), which is the only CAI age currently available in the literature calculated with a measured $^{238}\text{U}/^{235}\text{U}$ ratio. Pooling the ages we obtained for Efremovka CAIs with that of the SJ101 CAI from Allende yields a weighted mean age of 4567.30 ± 0.16 My, suggesting that the time scale of the CAI-forming event inferred from our absolute chronology may be as short as 160,000 years. Therefore, these data collectively support a single and brief time interval for the formation of CV CAIs, in agreement with the rapid time scales of less than 50,000 years required for their condensation and evaporative melting based on bulk $^{26}\text{Al}-^{26}\text{Mg}$ systematics (6, 13). However, our preferred age for the CAI-forming event and, by extension, the formation of the solar system, is based on the best-constrained age of 4567.35 ± 0.28 My obtained for the 22E CAI (Fig. 2A). This interpretation is founded on the petrographic features of this inclusion, suggesting an origin as a gas-solid condensate,

Table 1. Summary of Pb-Pb ages, $^{238}\text{U}/^{235}\text{U}$ ratios used in age calculations, and ^{54}Cr compositions of individual CAIs and chondrules. The Pb concentrations are based on the total amount of Pb analyzed. $\mu = ^{238}\text{U}/^{204}\text{Pb}$. The $\epsilon^{54}\text{Cr}$ values represent 10^4 deviation of the $^{54}\text{Cr}/^{52}\text{Cr}$ value of a sample relative to the terrestrial chromium reference standard and were acquired following Trinquier *et al.* (41). Uncertainties reflect the external reproducibility of 9 ppm. The $\epsilon^{54}\text{Cr}$ value for the 31E CAI is from Larsen *et al.* (13).

Sample	Type	Weight (mg)	μ	Pb (ppb)	Age (My)	$^{238}\text{U}/^{235}\text{U}$	$\epsilon^{54}\text{Cr}$
22E	CAI	25.9	46	178.8	4567.35 ± 0.28	137.627 ± 0.022	
31E	CAI	57.6	247	119.4	4567.23 ± 0.29	137.770 ± 0.022	6.8 ± 1.2
32E	CAI	18.0	116	322.3	4567.38 ± 0.31	137.832 ± 0.022	
C30	Chondrule	29.7	246	24.1	4567.32 ± 0.42	137.786 ± 0.013	-0.58 ± 0.09
C1	Chondrule	30.0	23	78.3	4566.67 ± 0.43	137.786 ± 0.013	-0.60 ± 0.09
C20	Chondrule	28.5	26	40.8	4566.24 ± 0.63	137.786 ± 0.013	-0.36 ± 0.09
C3	Chondrule	107.6	183	27.6	4566.02 ± 0.26	137.786 ± 0.013	-0.87 ± 0.09
C2	Chondrule	58.9	63	77.7	4564.71 ± 0.30	137.786 ± 0.013	-0.24 ± 0.09

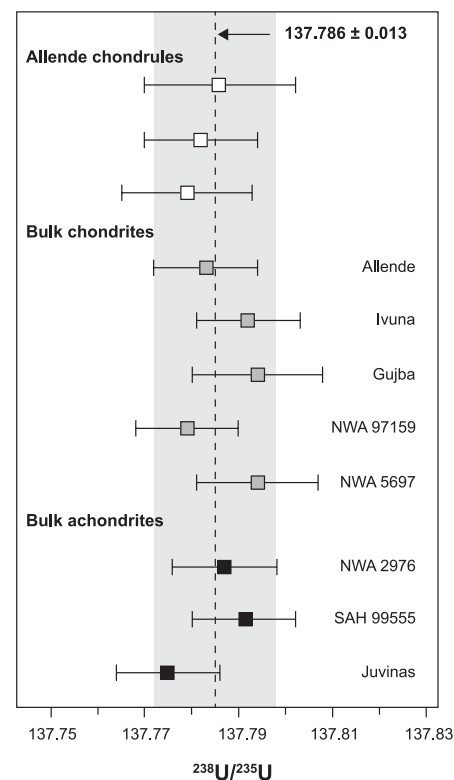


Fig. 1. $^{238}\text{U}/^{235}\text{U}$ ratios of individual chondrules, bulk chondrites, and achondrites. These samples define a mean of 137.786 ± 0.013 [mean square of weighted deviations (MSWD) = 1.2], which we interpret as the present-day solar $^{238}\text{U}/^{235}\text{U}$ ratio. The vertical gray band reflects the 2 SD uncertainty of the $^{238}\text{U}/^{235}\text{U}$ solar value. Uncertainties of sample measurements reflect external reproducibility or the internal precision of individual analyses, whichever is larger.

together with the combined effect of the slightly smaller errors on the age due to the greater spread in Pb-Pb data to define the $^{207}\text{Pb}_R/^{206}\text{Pb}_R$ ratio, greater number of points defining the isochron, acceptable sample/blank ratios for all measure-

ments used to define the array (table S4), and the low amount of terrestrial Pb contamination (21).

Because of the lack of $^{238}\text{U}/^{235}\text{U}$ variability among bulk inner solar system reservoirs, including three individual chondrules from the

Allende meteorite (Fig. 1), we used the well-constrained solar $^{238}\text{U}/^{235}\text{U}$ value of 137.786 ± 0.013 to calculate the absolute Pb-Pb ages of our subset of chondrules. In contrast to the narrow age span defined by CAIs, the chondrule ages

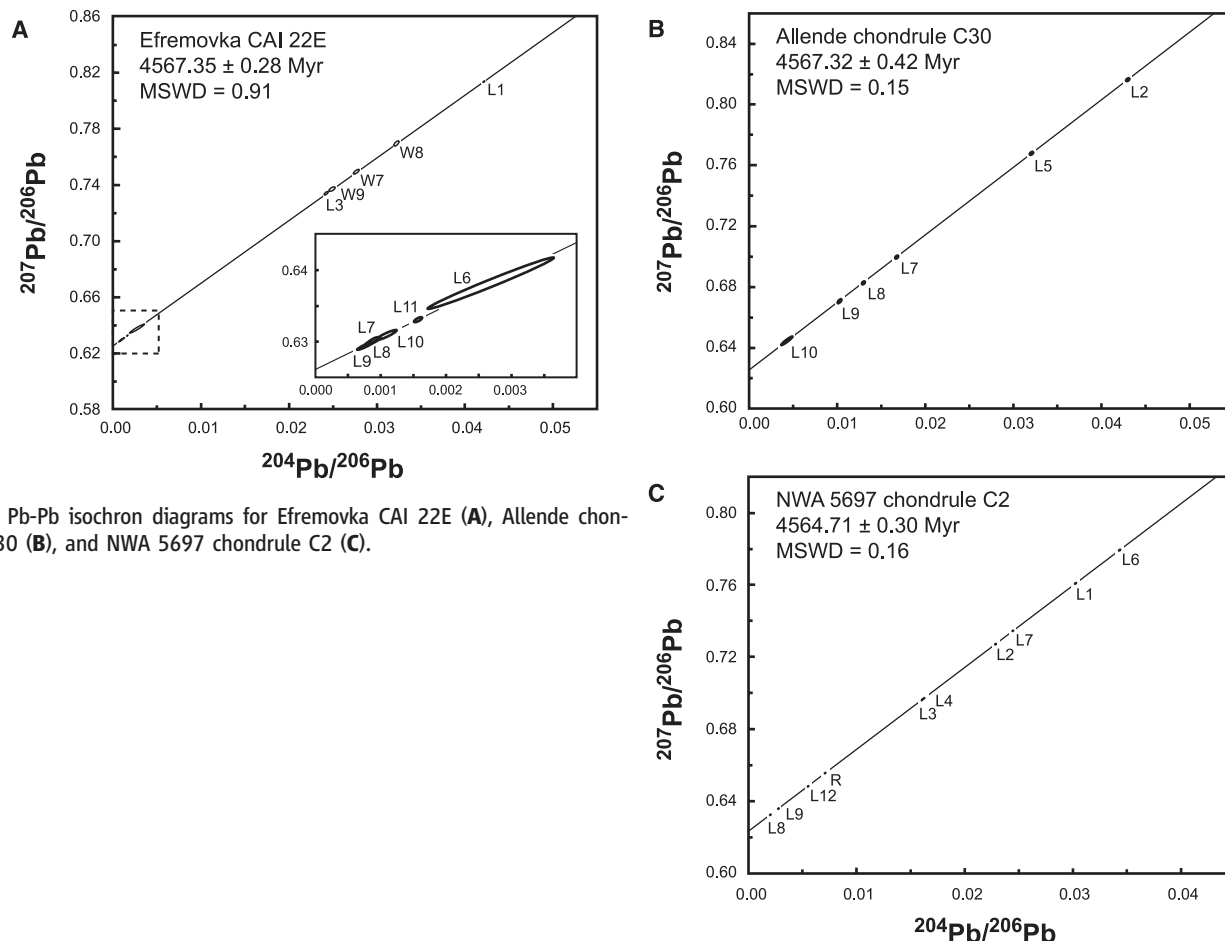
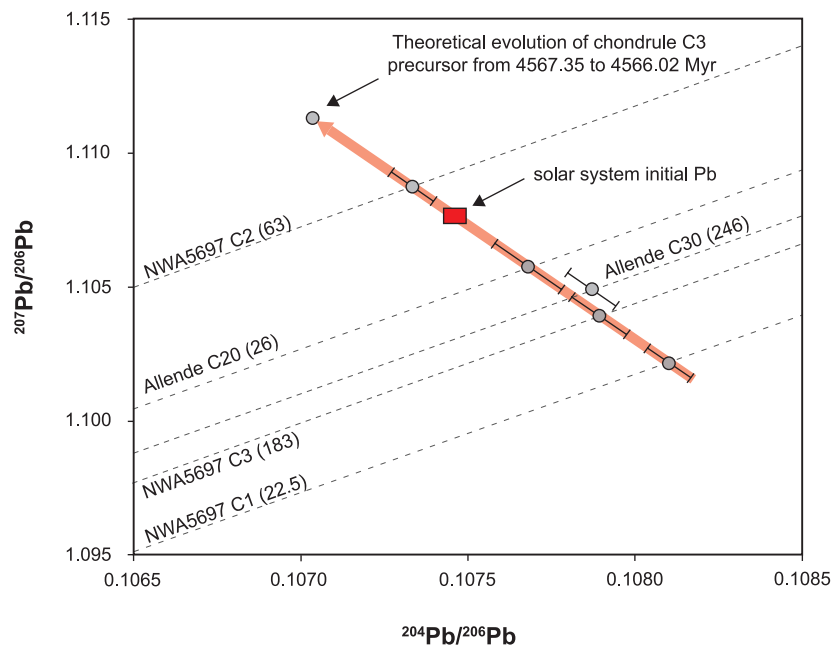


Fig. 2. Pb-Pb isochron diagrams for Efremovka CAI 22E (A), Allende chondrule C30 (B), and NWA 5697 chondrule C2 (C).

Fig. 3. Initial Pb isotopic compositions of individual chondrules. The initial Pb isotope compositions are defined by the intersection of the individual isochrons and a Pb evolution array anchored on the solar system initial Pb isotope composition defined by the Nantan iron meteorite (14). The μ values ($^{238}\text{U}/^{204}\text{Pb}$) of chondrules are indicated in parentheses. Chondrule C30 was displaced to the right-hand side of the solar system initial Pb array for clarity. The uncertainty of the solar system initial Pb value is smaller than the symbol.



range from 4567.32 ± 0.42 My to 4564.71 ± 0.30 My (Fig. 2, B and C, and Table 1). The oldest chondrule age overlaps with our estimate of CAI formation and thus requires that aggregation of the chondrule precursor material and its thermal processing occurred within the uncertainty of its Pb-Pb age. Moreover, the age of the oldest chondrule indicates that it was not heated to temperatures above the Pb closure temperature after 4567.32 ± 0.42 My and therefore has a formation and thermal history indistinguishable from that of CAIs. These data demonstrate that chondrule formation started contemporaneously with CAIs (within the uncertainty of our measurements) and continued for at least ~3 My.

The majority of chondrules are believed to have formed as dust aggregates of near-solar composition subsequently thermally processed by a flash heating mechanism creating the igneous textures we observe today (10). However, the presence of relict grains, igneous rims, and compound chondrules suggests that some chondrules may have grown by collisions and remelting (22, 23). Given the low solar $^{238}\text{U}/^{204}\text{Pb}$ ratio (μ) of ~0.15 (24), the Pb isotopic composition of a chondrule precursor is not expected to evolve measurably during the lifetime of the protoplanetary disk (~3 My) until its μ value is increased by Pb devolatilization during thermal processing. As such, internal isochron relationships of chondrules are expected to project back to nonevolved initial Pb isotopic compositions, unless an object experienced a complex

thermal history involving multiple heating and melting events. The isochron for the oldest Allende chondrule (C30) projects back to an initial Pb isotopic composition that is less radiogenic than the most primitive estimate of the initial Pb isotopic composition of the solar system (Fig. 3), based on the Nantan iron meteorite (14). The low μ value of the precursor material for chondrules in general and the antiquity of this chondrule in particular indicate that the Pb isotopic composition of the Nantan iron meteorite does not represent the initial Pb isotopic composition of the solar system, but instead an evolved composition inherited after accretion and differentiation of its parent body before core formation. Similar to chondrule C30, three of the four younger chondrules we analyzed define isochron relationships that project back to Pb isotopic compositions that are more primitive than the current estimate of the solar system initial Pb composition. This implies that the precursor material of these chondrules, especially C3 with its high μ value of ~183, were not thermally processed until at or near the derived Pb-Pb age. Thus, the range of ages we observe for individual chondrules reflects primary ages associated with a chondrule-forming event and not secondary disturbance of the Pb-Pb chronometer. Only the youngest chondrule, C2, yields an isochron that projects to a more evolved Pb isotopic composition, requiring that this inclusion was thermally processed for the first time early enough to have accumulated

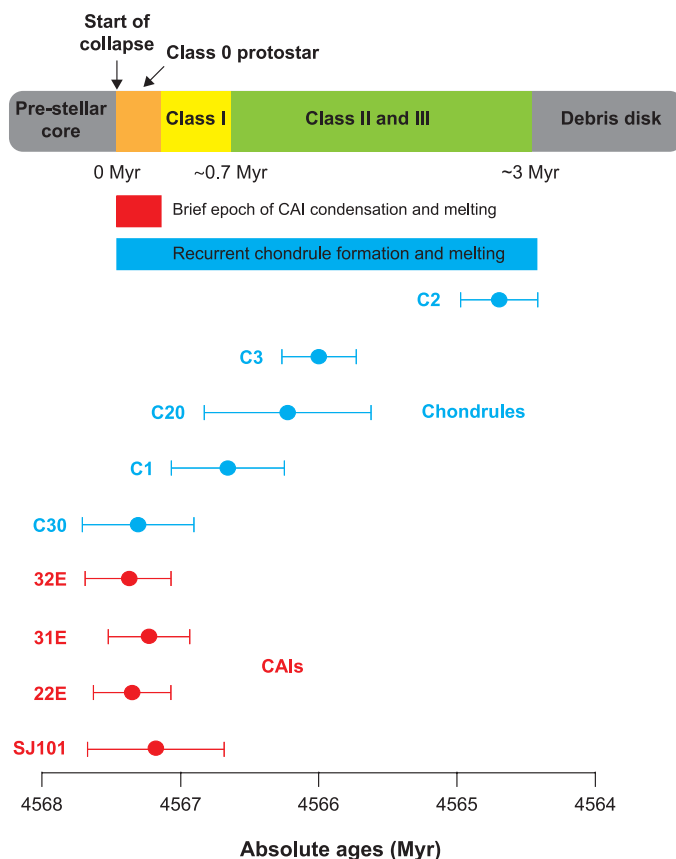
substantial radiogenic Pb by the time the last melting event occurred at 4564.71 ± 0.30 My.

Chondrules from the Allende and NWA 5697 chondrites define age ranges (Fig. 4) that indicate the presence of multiple generations of chondrules in individual chondrite groups. To explore the spatial significance of this age range, we have measured the $^{54}\text{Cr}/^{52}\text{Cr}$ ratios of these chondrules, because $^{54}\text{Cr}/^{52}\text{Cr}$ variations within the inner solar system track genetic relationships between early-formed solids and their respective reservoirs (25). The five chondrules analyzed here show significant ^{54}Cr variability (Table 1) that is not correlated with their ages. Moreover, most chondrules have $^{54}\text{Cr}/^{52}\text{Cr}$ ratios that are distinct from those of their host chondrites (26). Collectively, these observations indicate that chondrules from individual chondrite groups formed from isotopically diverse precursor material in different regions of the protoplanetary disk and were subsequently transported to the accretion regions of their respective parent bodies. This is consistent with the proposal that radial transport of material in the protoplanetary disk, such as by radial diffusion (27) and/or stellar outflows (3), was important during the epoch of CAI and chondrule formation (28).

Some models of chondrule formation such as current sheets (29), colliding molten planetesimals (30), and recycling of fragmented differentiated planetesimals (31) are based on the presumed offset of 1 to 2 My between the formation of CAIs and chondrules and therefore are inconsistent with the contemporaneous formation of CAIs and the oldest chondrules inferred from our study. Moreover, differentiated planetesimals typically have enhanced U/Pb values (32), which would result in chondrules with radiogenically evolved initial Pb isotopic compositions. However, the initial Pb isotopic composition of individual chondrules suggests that, in most cases, chondrule precursors retained the solar U/Pb value up to the chondrule-forming event(s).

Nebular shock waves are currently the favored mechanism for chondrule formation. The proposed sources of shock waves include infalling clumps of dust and gas (33), bow shocks generated by planetary embryos (34), spiral arms and clumps in a gravitationally unstable protoplanetary disk (35), and x-ray flares (3). Similar to the colliding planetesimals model, the formation of chondrules by bow shocks requires at least 1 My to allow for the growth of planetary embryos of adequate size and therefore cannot explain the existence of old chondrules. Accretion-driven shock models, including models based on a gravitationally unstable disk, require copious mass accretion rates to the central star on the order of $\sim 10^{-5}$ solar mass (M_{\odot}) year^{-1} to be plausible (36). Astronomical observations indicate that such high accretion rates are achieved only in the deeply embedded class 0 phase of star formation (37), and such accretion rates can only last for ~0.1 My. Thus, chondrule formation via accretion-driven

Fig. 4. Time scales of solid formation and disk evolution. The brief formation interval of 160,000 years for the CAI-forming event is similar to the median lifetimes of class 0 protostars of ~0.1 to 0.2 My inferred from astronomical observation of star-forming regions (37). Therefore, the thermal regime required for CAI condensation may only have existed during the earliest stages of disk evolution typified by high mass accretion rates ($\sim 10^{-5} M_{\odot} \text{year}^{-1}$) to the central star.



shocks is limited to the earliest stage of disk evolution. As such, different sources of shock waves would be required to account for the observed ~3 My age range of chondrule formation inferred from our study.

Our revised chronology of the formation of solids and their thermal processing refutes the long-held view of a time gap between the formation of CAIs and chondrules, thereby allowing for the possibility that the energy required for melting CAIs and chondrules may have been associated with the same physical process. Statistical studies based on astronomical observations of young stellar objects within star-forming regions indicate that the median lifetime of disks around low-mass stars is ~3 My (37). These time scales are comparable to the timing of melting of disk solids inferred from our Pb-Pb dates (Fig. 4), suggesting that the formation of CAIs and chondrules may reflect a process intrinsically linked to the secular evolution of protoplanetary disks (38) and is not unique to our solar system. Transfer of mass from the disk to the central protostar is the most energetic process during the lifetime of the protoplanetary disk. Although the energy generated during this process is only gradually released, part of which is converted into kinetic energy expressed as magnetically driven bipolar outflows from the protostar (39), a substantial amount of it is available for the thermal processing of solids during transient mass-accretion events. Indeed, models of the innermost structure of protoplanetary disks predict temperatures in excess of 1400 K within 1 astronomical unit for mass accretion rates as low as $\sim 10^{-6} M_{\odot} \text{ year}^{-1}$ (40). Because the conservation of energy requires dissipation per unit of area of the disk that scales as the inverse cube of the distance from the central star, accretion-based processes may produce similar thermal regimes over a large range of accretion rates, albeit at different orbital radii. Whether accretion-based processes can provide thermal histories for CAIs and chondrules that are consistent with their heating and cooling rates, as well as the chronology provided here, requires robust numerical simulations of the evolving thermal structure of accreting disks.

References and Notes

1. T. Lee, D. A. Papanastassiou, G. J. Wasserburg, *Astrophys. J.* **211**, L107 (1977).
2. C. Göpel, G. Manhès, C. J. Allègre, *Meteoritics* **26**, 338 (1991).
3. F. H. Shu, H. Shang, T. Lee, *Science* **271**, 1545 (1996).
4. A. Galy, E. D. Young, R. D. Ash, R. K. O'Nions, *Science* **290**, 1751 (2000).
5. Y. Amelin, A. N. Krot, I. D. Hutcheon, A. A. Ulyanov, *Science* **297**, 1678 (2002).
6. M. Bizzarro, J. A. Baker, H. Haack, *Nature* **431**, 275 (2004).
7. C. M. Alexander, J. N. Grossman, D. S. Ebel, F. J. Ciesla, *Science* **320**, 1617 (2008).
8. J. N. Connelly, Y. Amelin, A. N. Krot, M. Bizzarro, *Astrophys. J.* **675**, L121 (2008).
9. G. J. MacPherson, *Treatise on Geochemistry, Volume 1*, A. M. Davis, Ed. (Elsevier, Amsterdam, 2003), pp. 201–246.
10. E. R. D. Scott, *Annu. Rev. Earth Planet. Sci.* **35**, 577 (2007).
11. A. N. Krot et al., *Geochim. Cosmochim. Acta* **73**, 4963 (2009).
12. N. T. Kita et al., in *Chondrites and the Protoplanetary Disk*, A. N. Krot, E. R. D. Scott, B. Reipurth, Eds. (Astronomical Society of the Pacific, San Francisco, 2005), vol. 341, pp. 558–587.
13. K. K. Larsen et al., *Astrophys. J.* **735**, L37 (2011).
14. J. Blüchert-Toft, B. Zanda, D. S. Ebel, F. A. Albarède, *Earth Planet. Sci. Lett.* **300**, 152 (2010).
15. G. A. Brennecka et al., *Science* **327**, 449 (2010).
16. Materials and methods are available as supplementary materials on Science Online.
17. C. H. Stirling, A. N. Halliday, D. Porcelli, *Geochim. Cosmochim. Acta* **69**, 1059 (2005).
18. J. B. Blake, D. N. Schramm, *Nature* **289**, 138 (1973).
19. Y. Amelin et al., *Earth Planet. Sci. Lett.* **300**, 343 (2010).
20. M. Asplund, N. Grevesse, J. A. Sauval, P. Scott, *Annu. Rev. Astron. Astrophys.* **47**, 481 (2009).
21. Confidence in this age is also enhanced by the fact that the well-constrained isochron projects to an initial Pb isotopic composition that is more consistent with an initial Pb component from the CAI source reservoir than a modern terrestrial contamination (supplementary materials text 2).
22. A. N. Krot, J. T. Wasson, *Geochim. Cosmochim. Acta* **59**, 4951 (1995).
23. R. H. Jones, J. N. Grossman, A. E. Rubin, in *Chondrites and the Protoplanetary Disk*, A. N. Krot, E. R. D. Scott, B. Reipurth, Eds. (Astronomical Society of the Pacific, San Francisco, 2005), vol. 341, pp. 251–285.
24. H. Palme, A. Jones, in *Treatise on Geochemistry, Comets and Planets*, A. M. Davis, Ed. (Elsevier-Pergamon, Oxford, 2003), pp. 41–61.
25. A. Trinquier et al., *Science* **324**, 374 (2009).
26. A. Trinquier, J.-L. Birck, C. G. Allègre, *Astrophys. J.* **655**, 1179 (2007).
27. F. J. Ciesla, *Science* **318**, 613 (2007).
28. D. Brownlee et al., *Science* **314**, 1711 (2006).
29. M. K. Ryan Joung, M.-M. Mac Low, D. S. Ebel, *Astrophys. J.* **606**, 532 (2004).
30. E. Asphaug, M. Jutzi, N. Movshovitz, *Earth Planet. Sci. Lett.* **308**, 369 (2011).
31. G. Libourel, A. N. Krot, *Earth Planet. Sci. Lett.* **254**, 1 (2007).
32. J. N. Connelly, M. Bizzarro, K. Thrane, J. A. Baker, *Geochim. Cosmochim. Acta* **72**, 4813 (2008).
33. A. P. Boss, J. A. Graham, *Icarus* **106**, 168 (1993).
34. S. J. Weidenschilling, F. Marzari, L. L. Hood, *Science* **279**, 681 (1998).
35. A. P. Boss, R. H. Durisen, *Astrophys. J.* **621**, L137 (2005).
36. E. I. Vorobyov, S. Basu, *Astrophys. J.* **719**, 1896 (2010).
37. N. J. Evans II et al., *Astrophys. J.* **181** (suppl.), 321 (2009).
38. R. Salmeron, T. R. Ireland, *Earth Planet. Sci. Lett.* **327–328**, 61 (2012).
39. C. Zanni, A. Ferrari, R. Rosner, G. Bodo, S. Massaglia, *Astron. Astrophys.* **469**, 811 (2007).
40. P. D'Alessio, N. Calvet, D. H. Woolum, in *Chondrites and the Protoplanetary Disk*, A. N. Krot, E. R. D. Scott, B. Reipurth, Eds. (Astronomical Society of the Pacific, San Francisco, 2005), pp. 353–372.
41. A. Trinquier, J.-L. Birck, C. G. Allègre, *J. Anal. At. Spectrom.* **23**, 1565 (2008).

Acknowledgments: All the data reported in this paper are presented in the supplementary materials. The Centre for Star and Planet Formation is financed by the Danish National Research Foundation. We thank C. Paton for help in the mass spectrometer laboratory and J. K. Jørgensen for discussion.

Supplementary Materials

www.sciencemag.org/cgi/content/full/338/6107/651/DC1
Materials and Methods
Supplementary Text
Figs. S1 to S22
Tables S1 to S4
References (42–55)

3 July 2012; accepted 14 September 2012
10.1126/science.1226919

Chloroplast Biogenesis Is Regulated by Direct Action of the Ubiquitin-Proteasome System

Qihua Ling,* Weihua Huang,*† Amy Baldwin,‡ Paul Jarvis§

Development of chloroplasts and other plastids depends on the import of thousands of nucleus-encoded proteins from the cytosol. Import is initiated by TOC (translocon at the outer envelope of chloroplasts) complexes in the plastid outer membrane that incorporate multiple, client-specific receptors. Modulation of import is thought to control the plastid's proteome, developmental fate, and functions. Using forward genetics, we identified *Arabidopsis* SP1, which encodes a RING-type ubiquitin E3 ligase of the chloroplast outer membrane. The SP1 protein associated with TOC complexes and mediated ubiquitination of TOC components, promoting their degradation. Mutant *sp1* plants performed developmental transitions that involve plastid proteome changes inefficiently, indicating a requirement for reorganization of the TOC machinery. Thus, the ubiquitin-proteasome system acts on plastids to control their development.

Chloroplasts belong to a family of plant organelles called plastids, which includes several nonphotosynthetic variants (such as

etioplasts in dark-grown seedlings and carotenoid-rich chromoplasts in fruits) (*1*). A specific feature of the plastid family is the ability to interconvert in response to developmental and environmental cues—for example, during de-etiolation or fruit ripening (*1*). Such plastid interconversions are linked to reorganization of the organellar proteome (*2, 3*).

Over 90% of the thousands of proteins in plastids are nucleus-encoded and imported from the cytosol posttranslationally (*1*). The translocon at the outer envelope of chloroplasts (TOC) recognizes chloroplast pre-proteins and initiates

Department of Biology, University of Leicester, Leicester LE1 7RH, UK.

*These authors contributed equally to this work.

†Present address: Shanghai Institute of Plant Physiology and Ecology, Shanghai Institutes for Biological Sciences, Chinese Academy of Sciences, Shanghai 200032, China.

‡Present address: School of Medicine, Cardiff University, Cardiff CF14 4YS, UK.

§To whom correspondence should be addressed. E-mail: rpj3@le.ac.uk